Cys-27 Variant of Human δ-Opioid Receptor Modulates Maturation and Cell Surface Delivery of Phe-27 Variant via Heteromerization*□S

Tarja T. Leskelä[‡1], **Jarkko J. Lackman**[‡2], **Miia M. Vierimaa**[‡], **Hiroyuki Kobayashi**[§], **Michel Bouvier**[§3], **and Ulla E. Petäjä-Repo**[‡4]

From the ‡Department of Anatomy and Cell Biology, Institute of Biomedicine, University of Oulu, FI-90014 Oulu, Finland and the §Department of Biochemistry, Institute for Research in Immunology and Cancer, and Groupe de Recherche Universitaire sur le Médicament, Université de Montréal, Montréal, Québec H3C 3J7, Canada

Background: Human δ-opioid receptor (hδOR) carries F27C polymorphism in its extracellular domain.
Results: HδOR-Cys-27 with inherently impaired maturation/intracellular trafficking forms heteromers with hδOR-Phe-27 in the endoplasmic reticulum and enhances its targeting to degradation.
Conclusion: HδOR-Cys-27 impairs hδOR-Phe-27 cell surface delivery in a dominant negative manner.
Significance: Homo/heteromerization early in the biosynthetic pathway governs the levels of functionally active receptors at the cell surface.

The important role of G protein-coupled receptor homo/heteromerization in receptor folding, maturation, trafficking, and cell surface expression has become increasingly evident. Here we investigated whether the human δ-opioid receptor (hδOR) Cys-27 variant that shows inherent compromised maturation has an effect on the behavior of the more common Phe-27 variant in the early secretory pathway. We demonstrate that hδOR-Cys-27 acts in a dominant negative manner and impairs cell surface delivery of the co-expressed hδOR-Phe-27 and impairs conversion of precursors to the mature form. This was demonstrated by metabolic labeling, Western blotting, flow cytometry, and confocal microscopy in HEK293 and human SH-SY5Y neuroblastoma cells using differentially epitope-tagged variants. The hδOR-Phe-27 precursors that were redirected to the endoplasmic reticulum-associated degradation were, however, rescued by a pharmacological chaperone, the opioid antagonist naltrexone. Co-immunoprecipitation of metabolically labeled variants revealed that both endoplasmic reticulum-localized precursors and mature receptors exist as homo/heteromers. The existence of homo/heteromers was confirmed in living cells by bioluminescence resonance energy transfer measurements, showing that the variants have a similar propensity to form homo/heteromers. By forming both homomers and heteromers, the hδOR-Cys-27 variant may thus regulate the levels of receptors at the cell surface, possibly leading to altered responsiveness to opioid ligands in individuals carrying the Cys-27 variant.

The three opioid receptors, δ, κ, and μ, have a vital function in pain perception/modulation and analgesia (1). They belong to the family A G protein-coupled receptors (GPCRs)[5] and have a membrane topography that characterizes all GPCRs consisting of seven membrane-spanning domains with an extracellular N terminus and an intracellular C terminus. The human δ-opioid receptor (hδOR) has a common single-nucleotide polymorphism (T80G) that results in the replacement of phenylalanine (Phe) with cysteine (Cys) at the amino acid position 27 in the N-terminal domain of the receptor. The allelic frequency of the less common Cys-27 variant varies depending on the ethnic background and is around 10% in Caucasians (2, 3). Recently, we demonstrated that the Cys-27 variant shows an altered trafficking profile when expressed in HEK293 and CHO cells (4). The Cys-27 variant, but not the Phe-27 variant, shows compromised maturation and cell surface delivery. The receptor precursors, which are incapable of endoplasmic reticulum (ER) export, accumulate and are eventually targeted to ER-associated degradation (ERAD) (4). The ER-retained receptors, however, are not permanently misfolded, as they can be rescued to the plasma membrane by membrane-permeable opioid receptor pharmacological chaperones (5, 6).

In recent years it has become increasingly evident that opioid receptors do not exist only as monomers but form homomers and also heteromeric complexes with other opioid receptor subtypes and even with other GPCRs. This has been demonstrated using a number of biochemical and biophysical approaches such as co-immunoprecipitation and various resonance energy transfer techniques (see *e.g.* Refs. 7–16). These approaches utilizing heterologous expression systems have

been recently complemented by *in vivo* studies. For example, the existence of δ-κ and δ-μ heteromers has been demonstrated in CNS of rodents using heteromer-specific opioid ligands and antibodies, respectively (13, 17).

Opioid receptor heteromerization has been found to lead to pharmacological and functional diversity, as heteromers show altered ligand binding, signaling, and trafficking properties compared with the corresponding mono/homomers (for review, see Refs. 18 and 19). In contrast, much less is known about the functional significance of homomeric complexes. The family C, GPCRs, such as GABA_B receptors, exist as obligatory homo/heteromers that are formed shortly after synthesis in the ER (20). This notion has now been extended to family A GPCRs, and it has been suggested that homo/heteromerization might constitute a quality control step in the ER, predicting that proper receptor-receptor interactions are prerequisite for ER export and delivery to the plasma membrane (21). In support of this idea are the observations for an increasing number of naturally occurring GPCR slice variants and mutant forms as well as engineered receptor mutants that have been shown to behave as dominant-negatives of their corresponding wild-type forms by preventing their expression at the cell surface (*e.g.* rhodopsin (22) and D3 dopamine (23), D2 dopamine (24), gonadotropin-releasing hormone (25, 26), melanocortin-1 (27, 28), thyroid-stimulating hormone (29), luteinizing hormone (30), CCR5 chemokine (31, 32), and V2 vasopressin (33) receptors). On the other hand, a few family A GPCRs have been shown to promote cell surface delivery of other receptors. For instance, it was shown that the α_{1D}-adrenergic receptor requires interaction with the α_{1B}-adrenergic receptor for targeting to the cell surface (34). Even more direct evidence for a connection between receptor homo/heteromerization and ER export has emerged from recent studies in which homomerization-compromised receptor mutants were found to be retained intracellularly (35, 36). Whether homomerization (or heteromerization) is required for ER exit of opioid receptors as well is still an open question. Whereas a few studies suggest that opioid receptors form homo/heteromers intracellularly (11, 15), others argue that this takes place only at the cell surface (37).

Based on the divergent trafficking properties of the two hδOR variants (4), we set out to investigate whether the Cys-27 variant might alter trafficking of the Phe-27 variant in the early secretory pathway, possibly by forming heteromeric complexes in the ER. We show that the Cys-27 variant indeed acts in a dominant negative manner and impairs maturation and cell surface delivery of the Phe-27 variant. Furthermore, using co-immunoprecipitation of differentially tagged variants, the ER-localized precursors were found to exist as heteromers and the bioluminescence resonance energy transfer (BRET) technique revealed that the variants had a similar ability to form homo and heteromers. The F27C polymorphism may thus govern the levels of functionally active hδOR homo/heteromers at the cell surface.

EXPERIMENTAL PROCEDURES

DNA Constructs—The hδOR^Cys-27, hδOR^Phe-27, and the rat luteinizing hormone receptor (rLHR) constructs in the pFT-SMMF vector with a cleavable influenza HA signal peptide, an

N-terminal Myc-tag (EQKLISEEDL), and a C-terminal FLAG-tag (DYKDDDDK) have been described previously (4, 6, 38). The constructs encoding hδOR^Cys-27 and hδOR^Phe-27 with a HA signal peptide and an N-terminal HA-tag (YPYDVPDYA) in pcDNA3.1 and the corresponding hδOR^Cys-27 construct in pFT-SMMF have been described in Refs. 39 and 4, respectively.

Expression vectors encoding hδOR^Cys-27 and hδOR^Phe-27 fused to either the Venus variant of the enhanced YFP (40) or *Renilla reniformis* luciferase (*R*luc) were prepared for the BRET[1] experiments. In short, the HA-tagged hδOR^Cys-27 (4) was subcloned into a modified pcDNA3.1/Zeo^(+)-Venus vector using restriction enzymes NheI and AvrII in a way that the 3′ end of the hδOR^Cys-27 sequence was fused onto the 5′ end of Venus. This resulted in an in-frame fusion of hδOR^Cys-27 with the Venus tag separated by a seven-amino acid linker. The hδOR^Cys-27-*R*luc-pcDNA3.1/Zeo^(+) construct has been described previously (14). The corresponding vectors encoding hδOR^Phe-27 were created by the QuickChange site-directed mutagenesis kit (Stratagene) as described (4). The construct encoding the HA- and Venus-tagged type-2b GABA_B receptor (GABA_B-R2) that was used as a control has been described earlier (41).

Cell Culture and Transfections—Cells were maintained in DMEM supplemented with 10% FBS, 100 units/ml penicillin, 0.1 mg/ml streptomycin (complete DMEM) at 37 °C in a humidified atmosphere of 5% CO_2. If needed, the medium contained the appropriate selection antibiotics. The tetracycline inducible HEK293 cell line (HEK293_i) expressing the Myc- and FLAG-tagged hδOR^Cys-27 (6) was transfected with hδOR^Phe-27-pcDNA3.1 encoding the HA-tagged hδOR^Phe-27 with the Lipofectamine 2000 transfection reagent (Invitrogen) under Blasticidin S (4 μg/ml; InvivoGen), hygromycin (400 μg/ml; InvivoGen), and Geneticin (400 μg/ml; InvivoGen) selection. Two clones were isolated and selected expressing hδOR^Phe-27 at ~2 and 19 pmol/mg of membrane protein in the absence of tetracycline induced expression of hδOR^Cys-27. The latter clone was used for co-immunoprecipitation experiments (Fig. 6). The cells were plated on culture flasks or plates (5–6 × 10^6 cells to 75-cm^2 culture flasks or 100-mm plates or 2 × 10^6 cells to 25-cm^2 culture flasks) for experiments and cultured for 3 days in complete DMEM. The hδOR^Cys-27 expression was induced by adding tetracycline (0–500 ng/ml; Invitrogen) to the culture medium for various periods of time as indicated in the figure legends. The proteasomal inhibitor lactacystin (10 μM; Enzo Life Sciences) was added to the culture medium 6 h before cells were harvested (Fig. 3*B*). For Western blotting and pulse-chase labeling experiments, cells were incubated in PBS, 20 mM *N*-ethylmaleimide for 10 min before harvesting, quick-frozen in liquid nitrogen, and stored at −70 °C.

The Flp-in-293 cells (Invitrogen) and human SH-SY5Y neuroblastoma cells (a kind gift of Dr. Mikko Hiltunen, University of Eastern Finland, Kuopio, Finland) were plated on 100-mm (2–4.5 × 10^6 cells) or 6-well (3 × 10^5 cells) culture plates and cultured for 24 h before transfection with hδOR or rLHR constructs. The medium was changed to Opti-MEM (Invitrogen), 4% (w/w) FBS 3 h before transfection. The DNA constructs (1–8 μg) and the Lipofectamine 2000 transfection reagent were incubated in Opti-MEM for 5 min, mixed (the mixture had a

final DNA:Lipofectamine ratio of 1:3), and incubated for another 20 min before adding the mixture to the cells (Figs. 4 and 5, *D–F*, supplemental Figs. 1*A* and 2). An alternative method was occasionally used for immunofluorescence microscopy to increase the number of transfected cells expressing only one receptor construct. For this purpose, each DNA construct was mixed with the transfection reagent separately before adding the mixtures to the cells (supplemental Fig. 1, *B–D*). In some cases cells transfected with the two methods were mixed before plating them to coverslips (Fig. 5, *A–C*). The amount of total DNA was kept constant with the appropriate vector DNA in experiments with varying amounts of constructs. The medium was changed to complete DMEM after 4 h, and cells were harvested or fixed 20 h later.

The HEK293 cells that were used for BRET[1] experiments were plated on 6-well plates (3×10^5 cells), cultured for 24 h in complete DMEM without selection antibiotics, and transfected with increasing amounts of receptor-*R*luc and receptor-Venus constructs. Polyethyleneimine (Polysciences Inc.) was used as the transfection reagent in a ratio of 3:1 (DNA (μg):polyethyleneimine). The amount of total DNA (2.1 μg) was kept constant with the appropriate vector DNA. After 24 h, the medium was changed for complete DMEM, and the cells were harvested 24 h later.

BRET[1] Assay—The transfected cells were washed with PBS containing 5 mM EDTA, detached, and resuspended in PBS. After quantifying the amount of protein by the Bio-Rad DC protein assay, the cells (2 μg) were distributed on 96-well plates (gray plates; PerkinElmer Life Sciences), and the total fluorescence was measured using the FlexStation IV (Molecular Devices) with excitation and emission filters set at 485 and 538 nm, respectively. The cells were then transferred to white 96-well plates (Corning), and the luciferase substrate coelenterazine H (Invitrogen) was added at a final concentration of 5 μM. The BRET signal, defined as the ratio of light intensity emitted at 510–550 nm (Venus) over 460–500 nm (*R*luc), was measured using the Mithras LB 940 instrument (Berthold Technologies). The values were corrected by subtracting the background BRET signal, detected for the *R*luc-tagged constructs expressed alone. The BRET values were plotted as a function of the ratio of total fluorescence and luminescence.

Radioligand Binding Assays—The membrane protein amount used for the ligand binding assays was adjusted according to the receptor expression level, ranging from 5 to 60 μg and from 2 to 10 μg for one-point and saturation binding assays, respectively. Briefly, the cells were homogenized in a buffer containing 25 mM Tris-HCl, pH 7.4, 5 mM $MgCl_2$, 2 mM EDTA, 5 μg/ml leupeptin, 5 μg/ml soybean trypsin inhibitor, and 10 μg/ml benzamidine with a Polytron homogenizer (Ultra-Turrax T-25; Ika) using 5-s bursts at 19,000 rpm. The membranes were separated by a series of centrifugation steps as described (4, 6). The binding assays were performed as described (4, 6) using [15,16-³H]diprenorphine (50.0–54.9 Ci/mmol, PerkinElmer Life Sciences) as a radioligand. For saturation binding assays, the final concentration of [³H]diprenorphine ranged from 0.06 to 16.5 nM. The triplicate samples of the one-point binding assay contained 10 nM [³H]diprenorphine.

Metabolic Labeling—The stably transfected HEK293$_i$ cells were pretreated with 500 ng/ml tetracycline for 1 or 16 h or were left untreated. The cells were then incubated in the depletion medium (methionine and cysteine-free DMEM) for 60 min and labeled for 40 min in the same medium containing 75–150 μCi/ml [³⁵S]methionine/cysteine (Easytag Express ³⁵S-protein labeling mix, 1175 Ci/mmol, PerkinElmer Life Sciences). The cells were washed twice with the chase medium (DMEM supplemented with 5 mM methionine) and chased for different periods of time as indicated in the figures. The opioid antagonist naltrexone (10 μM; Tocris) was added to the medium at the beginning of induction, and lactacystin (10 μM) at the beginning of depletion and were maintained thereafter.

Preparation of Whole Cell Extracts and Immunoprecipitation of Solubilized Receptors—Total cellular lysates were prepared in 0.5% (w/v) *n*-dodecyl-β-D-maltoside (Enzo Life Sciences), 25 mM Tris-HCl, pH 7.4, 140 mM $NaCl_2$, 2 mM EDTA, 5 μg/ml leupeptin, 5 μg/ml soybean trypsin inhibitor, and 10 μg/ml benzamidine, and the solubilized receptors were immunoprecipitated by one or two-step immunoprecipitation using the FLAG M2 or HA antibody affinity resins (both from Sigma) and eluted in SDS-sample buffer as described previously (6, 42). Mouse IgG (Sigma) was used as a control in the second immunoprecipitation step. Transferrin receptors were purified with the human transferrin receptor antibody (1:100; Zymed Laboratories Inc.) by two-step immunoprecipitation following a technique described earlier (42). The purified transferrin receptors in SDS-sample buffer (50 μl) were reduced with 10 μl of 0.2 M DTT (95 °C, 5 min) and alkylated with 10 μl of 0.5 M iodoacetamide (37 °C, 30 min).

Deglycosylation of Immunoprecipitated Receptors—Deglycosylation of immunoprecipitated receptors was performed using endo-β-*N*-acetylglucosaminidase H or peptide *N*-glycosidase F (both from Roche Applied Science) as described (6).

SDS-PAGE and Western Blotting—Samples were separated on SDS-PAGE using 7 or 10% SDS-polyacrylamide gels (6). The separated proteins were electroblotted, and the blots were probed with FLAG M2 (0.5 μg/ml, Sigma), HA (HA-7, 0.12 μg/ml, Sigma), and ubiquitin (1:1000, Enzo Life Sciences) antibodies (6). The SDS-PAGE gels containing radioactively labeled proteins were treated for fluorography (42), and films were scanned with the Umax PowerLook 1120 color scanner and the Image Master 2D Platinum 6.0 software. Data were quantified and analyzed as described (38).

Flow Cytometry—Cell surface receptors expressed in stably transfected HEK293$_i$ or in transiently transfected SH-SY5Y cells were analyzed by flow cytometry as described earlier (43) using c-Myc 9E10 (2 μg/ml; Santa Cruz) or HA (HA-7, 4 μg/ml; Sigma) antibodies and the phycoerythrin-conjugated rat anti-mouse IgG_1 secondary antibody (2 μg/ml; BD Biosciences). The fluorescence of live cells was measured with the BD Biosciences FACSCalibur flow cytometer, and the data were analyzed with CellQuestPro 6.0 as described (44). For the analysis of transiently transfected cells, the mean fluorescence of live cells minus the mean fluorescence of cells stained only with the secondary antibody was used for calculations.

Immunofluorescence—SH-SY5Y and Flp-in-293 cells were transiently transfected as described above, and after 4 h of

transfection, 2.5×10^6 cells were plated onto poly-L-lysine-coated coverslips in 12-well plates and cultured for 20 h in complete DMEM. Cells were fixed, permeabilized, and stained as described elsewhere (4). The primary antibodies were anti-HA (HA-7, 5 μg/ml; Y-11, 2 μg/ml, Santa Cruz), anti-cMyc (A-14, 1 μg/ml, Santa Cruz), anti-calreticulin (1:1000; Enzo Life Sciences), anti-Sec61β (1:500; Millipore), anti-ER-Golgi intermediate compartment (ERGIC)-53 (1:500; Alexis), and anti-GM130 (1:500; BD Biosciences). Alexa Fluor® 488 goat anti-mouse and Alexa Fluor® 568 goat anti-rabbit (1:250, Invitrogen) were used as secondary antibodies. Additionally, the nuclei were labeled with TO-PRO®-3 iodide (1:800, Invitrogen) for 10 min at 20 °C before final washes and mounting. The samples were viewed with the Zeiss LSM510 confocal microscope using the Zeiss Plan-Apo 100 × 1.4 NA oil immersion objective under the 488- and 647-nm wavelength excitation. The RGB profile plot analysis was performed with the ImageJ RBG profile plot plugin.

Data Analysis—Data were analyzed using the GraphPad Prism 4.02 software. The one-site binding and sigmoidal dose response models of the nonlinear regression analysis were used for the BRET data and the receptor maturation data in the metabolic labeling experiments, respectively. Statistical analyses were performed using the Student's *t* test for the comparisons between two groups or the one-way analysis of variance followed by the Bonferroni's multiple comparison test for multiple comparisons. The limit of significance was set as at $p < 0.05$. The data are presented as the mean ± S.E.

RESULTS

Co-expression of hδOR^Cys-27^ and hδOR^Phe-27^ in Stably Transfected HEK293 Cells Leads to Decrease in Expression of Mature hδOR^Phe-27^ at Cell Surface—To investigate whether hδOR^Cys-27^ has an effect on biosynthesis and trafficking of hδOR^Phe-27^, the variants were co-expressed in stably transfected HEK293 cells. A HEK293$_i$ cell line that expresses the N-terminally Myc- and C-terminally FLAG-tagged hδOR^Cys-27^ (Myc-hδOR^Cys-27^-FLAG) in an inducible manner (4, 6) was stably transfected with a construct encoding hδOR^Phe-27^ with an N-terminal HA-tag (HA-hδOR^Phe-27^). The co-transfected cells allowed expression of hδOR^Phe-27^ at a constant level with increasing amounts of hδOR^Cys-27^ upon induction with tetracycline. A clonal cell line was isolated that expressed [³H]diprenorphine binding sites in the absence of tetracycline at 2.1 ± 0.4 pmol/mg of membrane protein with a K_d of 0.88 ± 0.15 nM ($n = 3$). In these conditions, without induction, the HA antibody detected one major HA-hδOR^Phe-27^ form of about 55 kDa and two smaller barely detectable ones of about 48 and 43 kDa on Western blots (Fig. 1, *A* and *E, lane 1*), whereas no Myc-hδOR^Cys-27^-FLAG species were detectable with the FLAG antibody (Fig. 1*C, lane 1*). The 55- and 48-kDa hδOR^Phe-27^ species represent mature receptor glycoforms carrying either two or one *N*-glycans, respectively (4, 44), and the 43-kDa receptor form is a biosynthetic intermediate, *i.e.* the precursor of the 55-kDa hδOR^Phe-27^ form, carrying two unprocessed high mannose type *N*-glycans (4, 44). The precursor of the 48-kDa mature receptor was not detectable on Western blots but was observed in metabolic pulse-chase labeling experiments (see Fig. 2*A*). Identification of the mature and

precursor receptor forms was verified by their divergent sensitivity to peptide *N*-glycosidase F and endo-β-*N*-acetylglucosaminidase H (Fig. 1*E, lanes 1–4*). The former deglycosylating enzyme cleaves both unprocessed and fully processed *N*-glycans, whereas the latter is able to remove only high mannose type *N*-glycans that are typical of ER-localized glycoproteins.

When the co-transfected HEK293$_i$ cells were induced to express the hδOR^Cys-27^ variant, there was a tetracycline concentration-dependent increase in [³H]diprenorphine binding sites (Fig. 1*G*), reaching a level of 37.1 ± 1.8 pmol/mg protein at 500 ng/ml (K_d 0.60 ± 0.02 nM; $n = 3$). Concomitantly, there was a comparable increase in the expression of Myc-hδOR^Cys-27^-FLAG detected with the FLAG antibody (Fig. 1*C*). The pattern of receptor species expressed was similar in the tetracycline-treated parental and co-transfected HEK293$_i$ cells (Fig. 1*C, lanes 6 and 5*, respectively; see also Fig. 1*E, lanes 5–8*) and was comparable with the receptor species identified for hδOR^Phe-27^. The relative amount of precursors were, however, substantially higher for hδOR^Cys-27^. This characteristic of the Cys-27 variant is independent of receptor expression level (Fig. 1*C* and Ref. 4), delineating its less efficient maturation and ER export. Importantly, co-transfection of the two variants led to a decrease in the amount of the mature 55-kDa HA-hδOR^Phe-27^ species that was accompanied by a reciprocal increase in the amount of the corresponding precursor form, leading to a significant decrease in the mature receptor/precursor ratio (Fig. 1*A*, compare *lanes 1 and 5*; Fig. 1*B*). No alteration in the mature receptor/precursor ratio was seen for Myc-hδOR^Cys-27^-FLAG in the co-transfected cells compared with the parental cell line expressing only the Cys-27 variant (Fig. 1*C*, compare *lanes 5 and 6*; Fig. 1*D*).

In accordance with the results obtained for the Phe-27 variant by Western blotting, there were changes in the number of cell surface receptors after co-expression of the two variants, as assessed by flow cytometry. Using the HA antibody that detects the extracellular N-terminal epitope of the hδOR^Phe-27^ variant, a significant decrease in the number of cell surface receptors was observed in cells treated with 500 ng/ml tetracycline (Fig. 1*F*). Thus, these results show that the hδOR^Cys-27^ variant has a dominant negative effect on expression of the co-expressed hδOR^Phe-27^ variant, causing a decrease in the number of mature cell surface receptors.

The Co-expressed hδOR^Cys-27^ Interferes with Maturation of hδOR^Phe-27^ Variant—The observed changes in the steady-state amount of hδOR^Phe-27^ precursors and cell surface mature forms upon co-expression of the hδOR^Cys-27^ variant suggest that the biosynthesis of the Phe-27 form was impaired by the co-expressed Cys-27 variant. To test this possibility more directly, metabolic pulse-chase labeling experiments were performed (Fig. 2). Cells were first treated with tetracycline to induce expression of the Cys-27 variant for 16 h or were left untreated. Thereafter, they were labeled with [³⁵S]methionine/cysteine for 40 min and chased for 0–4 h. Receptors were then purified by immunoprecipitation and analyzed by SDS-PAGE and fluorography. As seen in Fig. 2*A*, the major form of the Phe-27 variant at the end of the pulse was the 43-kDa precursor, which in time disappeared and was converted to the mature 55-kDa form. The processing of the precursors was, however, impaired in cells that co-expressed the Cys-27 variant. Whereas
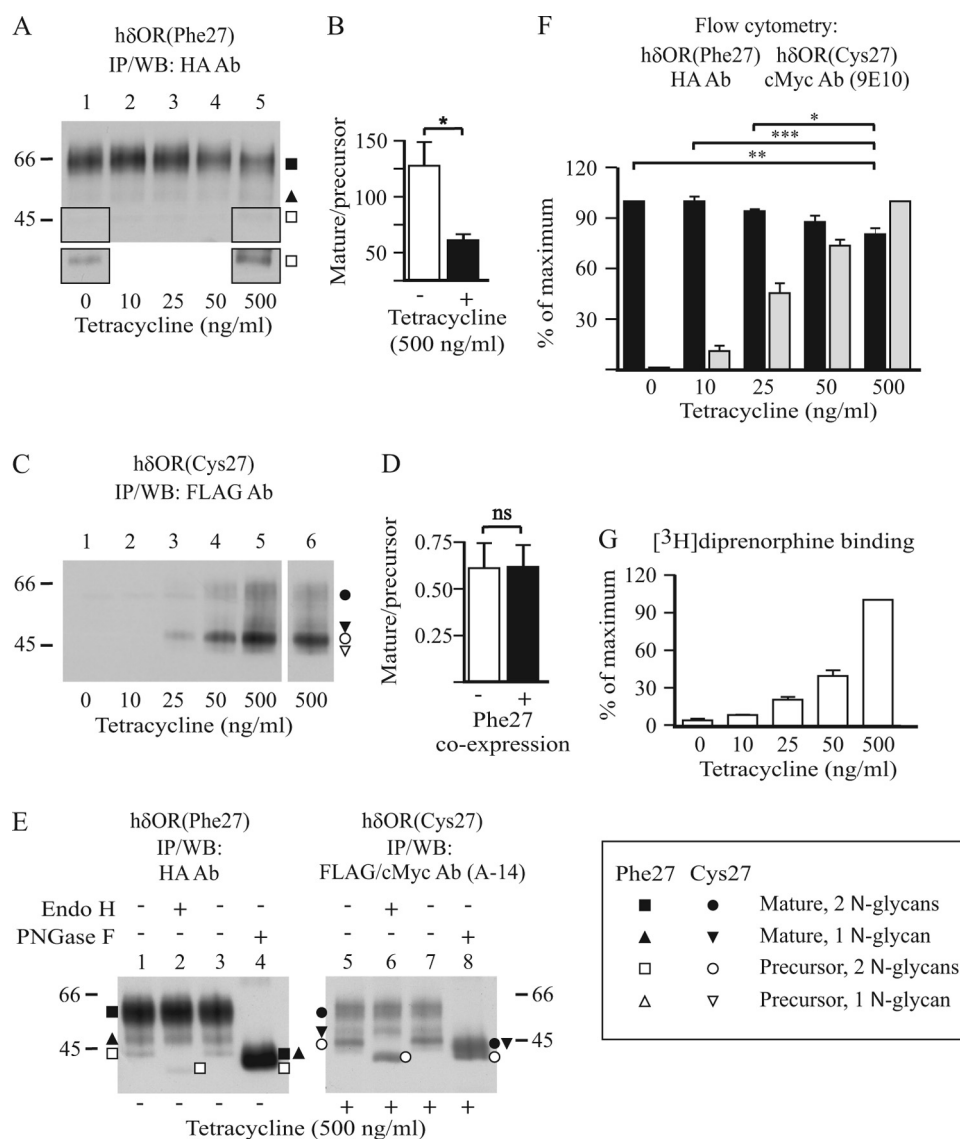
FIGURE 1. hδOR^{Cys-27} decreases expression of the mature hδOR^{Phe-27} variant at the cell surface in stably co-transfected HEK293$_i$ cells. *A–E*, HEK293$_i$ cells constitutively expressing HA-hδOR^{Phe-27} were induced or not with tetracycline for 24 h to express Myc-hδOR^{Cys-27}-FLAG. Receptors were purified from cellular lysates by immunoprecipitation with HA (*A*; *E, lanes 1–4*) or FLAG M2 (*C*; *E, lanes 5–8*) antibodies and subjected to deglycosylation with 50 milliunits/ml endo-β-N-acetylglucosaminidase H (*Endo H*; *E, lanes 2 and 6*) or 50 units/ml peptide *N*-glycosidase F (*PNGaseF*; *E, lanes 4 and 8*) or were left untreated (*E, lanes 1*, 3, 5, and 7). Samples were analyzed by SDS-PAGE and Western blotting (*WB*) using the indicated antibodies. In panel *A*, a longer exposure is shown for the outlined squared area of *lanes 1 and 5*. In panel *C*, *lane 6*, the parental HEK293$_i$ cells expressing only hδOR^{Cys-27} was used as a control. The blots were analyzed by densitometric scanning, and the mature receptor/precursor ratio for receptor glycoforms containing two *N*-glycans was calculated. The histograms in panels *B* and *D* represent the means ± S.E. of samples corresponding to *lanes 1 and 5* in panel *A* and *lanes 5 and 6* in panel *C*, respectively, from three independent experiments. The data were analyzed with the unpaired *t* test. Molecular weight markers are indicated on the *right* or *left* of the blots. The precursor and mature receptor forms are shown with *open* and *closed symbols*, respectively, as indicated. *F*, cell surface receptors were analyzed by flow cytometry using HA (*black bars*) and cMyc (*gray bars*) antibodies. The values shown are the means ± S.E. of four to five independent experiments performed in duplicate. The GeoMean values were normalized to those obtained from samples treated with 0 or 500 ng/ml tetracycline for hδOR^{Phe-27} and hδOR^{Cys-27}, respectively. The data were analyzed by Bonferroni's Multiple Comparison test after repeated measures one-way analysis of variance before normalization. *G*, the number of [^{3}H]diprenorphine binding sites was determined by one-point binding assays using cellular membranes. The B_{max} values were normalized to those obtained from cells treated with 500 ng/ml tetracycline and are shown as the means ± S.E. of two independent experiments. *ns*, not significant, *$p < 0.05$, **$p < 0.01$, ***$p < 0.001$.

almost all precursors had disappeared within 4 h in the non-induced cells, a substantial amount was still apparent in the induced cells (3.1 ± 1.3 and 10.8 ± 1.7% were left in the non-induced and induced cells, respectively, $p = 0.023$, $n = 3$). Concomitantly, less mature receptors were detected (compare *lanes 4 and 8* in Fig. 2*A*). Quantification of the fluorograms of the 2-h chase samples revealed that co-expression of the two variants led to a significant decrease in the hδOR^{Phe-27} mature receptor/precursor ratio (Fig. 2*E*). These changes were depen-

dent on the tetracycline concentration used to induce expression of the Cys-27 variant and were detectable already at the lowest concentration tested, 10 ng/ml (Fig. 2*B*). Although the maturation efficiency of hδOR^{Phe-27} was decreased, the kinetics of maturation appeared to be normal (Fig. 2*D*), suggesting that the hδOR^{Phe-27} precursors that are eventually able to leave the ER in the co-transfected cells mature normally. The transferrin receptor that is endogenously expressed in HEK293 cells showed no impaired maturation, as the ratio of the two immu-
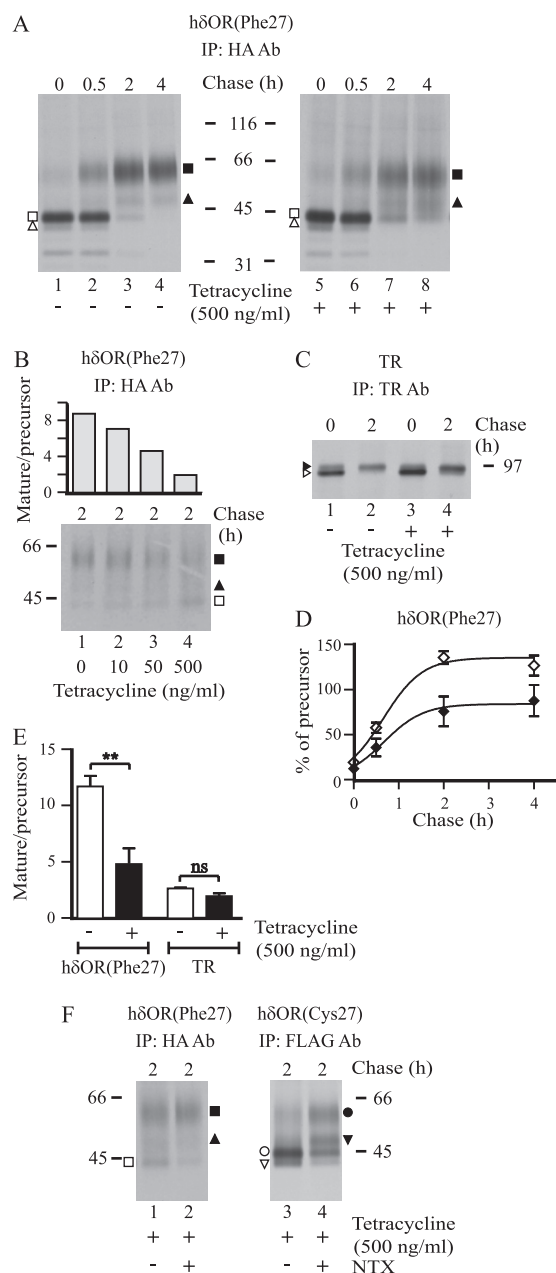
FIGURE 2. **hδOR^{Cys-27} impairs maturation of the hδOR^{Phe-27} variant in stably co-transfected HEK293$_i$ cells.** *A–C* and *F*, HEK293$_i$ cells constitutively expressing HA-hδOR^{Phe-27} were induced with tetracycline to express Myc-hδOR^{Cys-27}-FLAG for 16 h or were left untreated. In *panel F*, naltrexone (*NTX*; 10 μM) was added to the culture medium at the beginning of induction and was maintained thereafter. Cells were pulse-labeled with [^{35}S]methionine/cysteine for 40 min and chased for the indicated times. The hδOR^{Phe-27} and hδOR^{Cys-27} variants and the endogenously expressed transferrin receptors (*TRs*) were purified from lysates by two-step immunoprecipitation with HA, FLAG M2, and transferrin receptor antibodies, respectively, and analyzed by SDS-PAGE, fluorography and densitometric scanning of the fluorograms. In *panel D*, maturation curves are shown for hδOR^{Phe-27} with two *N*-glycans in non-induced (◇) and induced (◆) cells. The values are the means ± S.E. of three independent experiments normalized to the corresponding precursors at the end of the pulse. In *panel E* the mature receptor/precursor ratio for hδOR^{Phe-27} and TR was calculated from the 2-h chase samples. The values are the means ± S.E. of three to five independent experiments, analyzed by the unpaired *t* test. The precursor and mature hδOR forms are depicted with *open* and *closed symbols*, respectively, as specified in Fig. 1. The corresponding forms of the transferrin receptor are indicated with *arrowheads*. *ns*, not significant. **, $p < 0.01$.

noprecipitated receptor forms, the precursor and mature forms (45), was not changed significantly by hδOR^{Cys-27} expression in the 2-h chase samples (Figs. 2, *C* and *E*). This indicates that hδOR^{Cys-27} expression does not lead to general impairment in membrane protein biosynthesis. Furthermore, the co-expression did not lead to ER stress, as no differences in expression of the ER molecular chaperones BiP, ERp72, or protein-disulfide isomerase were detected, in contrast to what was observed for cells treated with tunicamycin (data not shown), a well known inducer of ER stress and the unfolded protein response.

Interestingly, the relative amount of Phe-27 variant glycoforms carrying only one *N*-glycan were increased in the induced *versus* the non-induced cells (Fig. 2*A*). The change was detected for both receptor precursor and mature forms. This suggests impairment in glycosylation of the nascent hδOR^{Phe-27}, *i.e.* less efficient co-translational addition of *N*-glycan to Asn-33 (44) when the two variants are co-expressed. In addition, the mature hδOR^{Phe-27}, whether carrying one or two *N*-glycans, migrated as less distinct bands on SDS-PAGE in cells co-expressing the Cys-27 variant (Fig. 2*A*), suggesting more heterogeneous processing of receptor-bound glycans in the Golgi. The changes in hδOR^{Phe-27} glycosylation were specific and did not result from a general impairment in protein glycosylation as no apparent changes were detected for the transferrin receptor (Fig. 2*C*), which is *O*-glycosylated and carries three *N*-glycans (45, 46).

Opioid Receptor Pharmacological Chaperone Enhances Maturation of Co-expressed hδOR Variants—Earlier studies have shown that membrane-permeable opioid antagonists can be used as pharmacological chaperones to enhance maturation of hδOR^{Cys-27} as well as hδOR^{Phe-27} when the variants are expressed individually (4–6). These ligands are able to bind to ER-localized precursors and enhance their folding and transport to the cell surface (6). Thus, we assessed whether the Cys-27 variant-mediated impairment in maturation of the Phe-27 variant could be overcome with a pharmacological chaperone. In a positive case, this would give further support to the notion that the Cys-27 variant alters the behavior of the Phe-27 variant early in the secretory pathway. The stably transfected HEK293$_i$ cells were induced to express Myc-hδOR^{Cys-27}-FLAG and were subjected to metabolic labeling in the absence or presence of 10 μM naltrexone, an opioid receptor-specific antagonist. The treatment led to a decrease in the amount of precursors and a concomitant increase in the amount of mature receptors (Fig. 2*F*). The latter change, however, was clearly apparent only for the Cys-27 variant. The increase in the amount of the mature hδOR^{Cys-27} carrying only one *N*-glycan was particularly evident, in line with our previous report (4).

Co-expression of hδOR Variants Leads to Increased Targeting of hδOR^{Phe-27} Precursors to ERAD—As the processing of hδOR^{Phe-27} precursors was compromised after co-expression of the Cys-27 variant, we next tested the possibility that the precursors that were not exported out of the ER are targeted to ERAD. To this end, non-induced and induced stably transfected HEK293$_i$ cells were treated with a specific proteasomal inhibitor lactacystin or vehicle and subjected to metabolic labeling. After a 2-h chase, the cells were harvested, and receptors were purified and analyzed. The lactacystin treatment stabilized the Myc-hδOR^{Cys-27}-FLAG precursors (compare *lanes*

FIGURE 3. **hδOR^{Cys-27} redirects hδOR^{Phe-27} precursors to ERAD in stably co-transfected HEK293$_i$ cells.** HEK293$_i$ cells constitutively expressing HA-hδOR^{Phe-27} were induced with tetracycline to express Myc-hδOR^{Cys-27}-FLAG for 16 h or were left untreated. *A*, cells were pulse-labeled with [^{35}S]methionine/cysteine for 40 min and chased for 2 h. Lactacystin (10 μM) or vehicle was added 60 min before labeling. The hδOR^{Phe-27} and hδOR^{Cys-27} variants were purified from lysates by two-step immunoprecipitation with the HA and FLAG M2 antibodies, respectively, and analyzed by SDS-PAGE and fluorography. *B*, alternatively, the variants were purified as described above by one-step immunoprecipitation from lysates of non-labeled cells that were treated or not with lactacystin for 6 h at the end of the 24-h induction. The purified samples were subjected to SDS-PAGE and Western blot (*WB*) analysis with the ubiquitin antibody. The precursor and mature receptor forms are indicated with *open* and *closed symbols*, respectively, as specified in Fig. 1. The *asterisks* depict polyubiquitinated receptors.

5 and 6 in Fig. 3*A*), consistent with previous results (4, 42). A similar stabilization of hδOR^{Phe-27} precursors was observed, but this was clearly seen only in cells expressing both variants (compare *lanes 3* and *4* to *lanes 1* and *2* in Fig. 3*A*). This suggests that hδOR^{Cys-27} co-expression leads to targeting of some of the hδOR^{Phe-27} precursors to ERAD. This conclusion was also supported by the finding that a slowly migrating high molecular weight smear at the top of the SDS-PAGE gels became apparent in the lactacystin-treated cells (Fig. 3*A*). This heterogeneous smear is likely to represent polyubiquitinated receptors that accumulate after proteasomal blockade (42). On Western blot analysis, the ubiquitin antibody was able to recognize a similar smear at the top of the gel when either the immunoprecipitated HA-hδOR^{Phe-27} or Myc-hδOR^{Cys-27}-FLAG was analyzed from the induced lactacystin-treated cells (Fig. 3*B*). Importantly, the high molecular weight polyubiquitinated forms of the hδOR^{Phe-27} variant were more apparent in induced *versus* non-induced cells even without the lactacystin treatment (Fig. 3*A*). Such diffuse high molecular weight species were also seen in the pulse-chase experiments shown in Fig. 2*A*.

hδOR^{Cys-27} Interferes with Maturation and Trafficking of hδOR^{Phe-27} in Human SH-SY5Y Neuroblastoma Cells—The results presented above suggest that hδOR^{Cys-27} that shows inherently impaired ER export, redirects some of the co-ex-

pressed hδOR^{Phe-27} precursors to ERAD, and thus lowers their maturation efficiency in co-transfected HEK293$_i$ cells. To rule out the possibility that these results were a peculiarity of HEK293 cells or the isolated stable cell line, we co-expressed the two variants in neuronal cells, human neuroblastoma SH-SY5Y cells that are known to express δORs endogenously (47). A Western blot analysis of immunoprecipitated receptors from cells transfected separately with Myc-hδOR^{Cys-27}-FLAG and HA-hδOR^{Phe-27} cDNA showed that the two variants were expressed as precursor and mature receptor forms in a similar manner as in the stably transfected HEK293$_i$ cells (Fig. 4*A*, *lanes 1* and *10*). The difference in the mature receptor/precursor ratio between the two variants was clearly evident, being even more apparent than in the HEK293 cells. This confirms that the low maturation efficiency of the Cys-27 variant is an inherent property of this variant and is clearly detected also in cells endogenously expressing the receptor. To assess the consequences of co-expression, the cells were transfected with a constant low amount (1 μg) of HA-hδOR^{Phe-27} cDNA and increasing amounts of Myc-hδOR^{Cys-27}-FLAG cDNA, reaching a ratio of 1:8. Receptor expression was then studied by immunoprecipitation and Western blotting or, alternatively, by flow cytometry. As seen in Fig. 4*A*, the amount of both mature receptors and precursors of hδOR^{Phe-27} decreased upon co-expression, already at a 1:1 plasmid ratio. A concomitant significant decrease in the number of cell surface receptors was detected by flow cytometry (Fig. 4*B*). No such changes were observed when Myc-rLHR-FLAG was co-expressed with HA-hδOR^{Phe-27} (Fig. 4, *C* and *D*), confirming that the changes observed were not due to general membrane protein overexpression. LHR is another family A GPCR that shows compromised ER export and maturation (38).

The Cys-27 variant-mediated impairment in maturation and cell surface expression of the Phe-27 variant appeared to be more apparent in the transiently transfected SH-SY5Y cells than in the stably transfected HEK293 cells. To verify that this was because of a different transfection system and not a cell line-specific phenomenon, Flp-in-293 cells were transiently co-transfected with Myc-hδOR^{Cys-27}-FLAG and HA-hδOR^{Phe-27} in a similar manner as in the case of the neuroblastoma cells. As expected, the Western blot analysis of the expressed receptors revealed results that were comparable with those obtained using the SH-SY5Y cells (supplemental Fig. 1*A*). Finally, we investigated whether the distinct epitope tags added to the two variants might have an effect on the observed changes in receptor behavior. For this purpose, we transfected the SH-SY5Y cells with receptor constructs harboring reciprocal epitope tags: N-terminal Myc-tagged and C-terminal FLAG-tagged hδOR^{Phe-27} and N-terminal HA-tagged hδOR^{Cys-27}. Again, the number of cell surface receptors of the hδOR^{Phe-27} variant was decreased after co-expression of the hδOR^{Cys-27} variant (data not shown).

The co-transfected SH-SY5Y cells were then subjected to immunofluorescence analysis to assess the subcellular localization of the two hδOR variants. As seen in Fig. 5, the Phe-27 variant was localized mainly at the cell surface, whereas the Cys-27 variant clearly showed more extensive intracellular staining. In the co-transfected cells, both variants accumulated
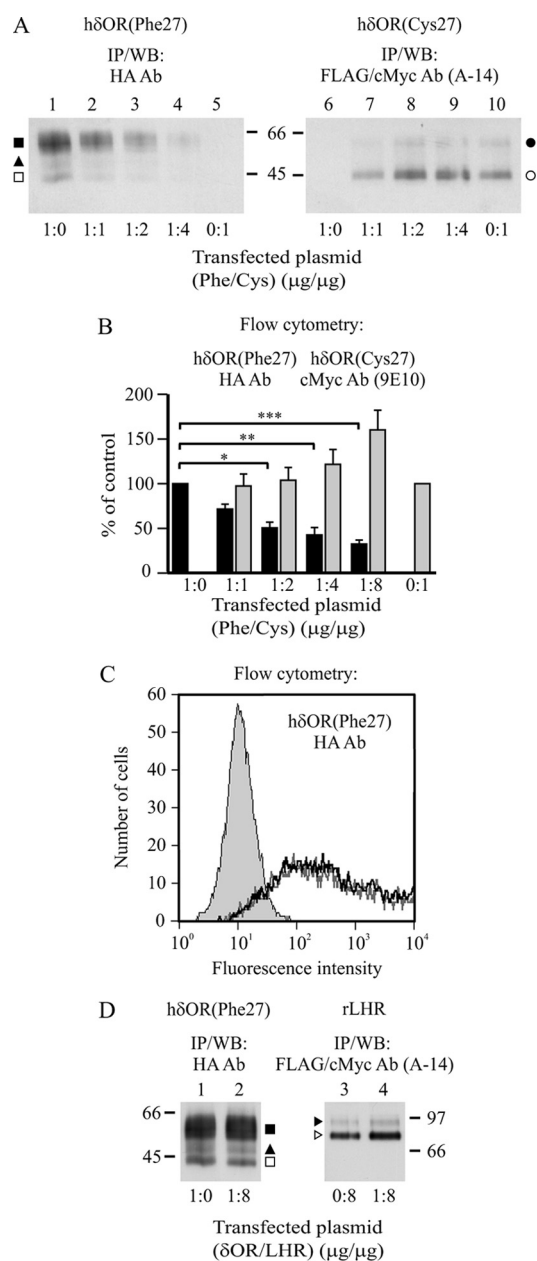
FIGURE 4. **hδOR^{Cys-27} impairs maturation and cell surface expression of the hδOR^{Phe-27} variant in transiently co-transfected SH-SY5Y neuroblastoma cells.** SH-SY5Y cells were co-transfected with HA-hδOR^{Phe-27} and Myc-hδOR^{Cys-27}-FLAG for 24 h using various cDNA ratios as indicated (*A* and *B*). As a control, HA-hδOR^{Phe-27} was co-transfected with Myc-rLHR-FLAG (δOR/LHR, 1:8) (*C* and *D*). After 24 h, cells were analyzed by flow cytometry (*B* and *C*) or were lysed and subjected to immunoprecipitation, SDS-PAGE, and Western blotting (*WB*) using the indicated antibodies (*A* and *D*). The values shown in *panel B* (HA antibody, *black bars*; cMyc antibody, *gray bars*) are the means ± S.E. of two-three independent experiments. The GeoMean values were normalized to those obtained from cells that were transfected only with hδOR^{Phe-27} or hδOR^{Cys-27}. The data were analyzed by Bonferroni's Multiple Comparison test after repeated measures one-way analysis of variance before normalization. *, $p < 0.05$; **, $p < 0.01$; ***, $p < 0.001$. In *panel C*, the *shaded curve* represents the background signal obtained in the absence of the primary antibody. The *black* and *gray curves* correspond to hδOR^{Phe-27} in cells co-transfected with rLHR in δOR/LHR DNA ratio of 1:0 and 1:8, respectively. The precursor and mature hδOR forms in *panels A* and *D* are indicated with *open* and *closed symbols*, respectively, as specified in Fig. 1, and the LHR precursor and mature forms (38) in *panel D* are indicated with *open* and *closed arrowheads*, respectively.

in a perinuclear compartment that is likely to correspond to receptor precursors that are eventually targeted to ERAD. Similar results were obtained using Flp-in-293 cells (supplemental Fig. 1, *B–G*). In the co-transfected SH-SY5Y cells, the accumulating Phe-27 variant co-localized weakly with ER markers calreticulin and Sec61β and more strongly with ER-Golgi intermediate compartment and Golgi markers, ERGIC-53 and GM130, respectively (supplemental Fig. 2).

Both Precursor and Mature Forms of hδOR^{Cys-27} and hδOR^{Phe-27} Form Heteromers—The altered behavior of hδOR^{Phe-27} precursors upon co-expression of the Cys-27 variant would be consistent with the idea that the variants form heteromers early in the secretory pathway. To more directly test this hypothesis, a co-immunoprecipitation assay was applied using the stably transfected HEK293$_i$ cells. The cells were induced to express the Cys-27 variant, labeled with [^{35}S]methionine/cysteine and harvested either immediately after the pulse or, alternatively, after a 6-h chase. This allowed assessing directly whether precursors or mature forms or both are capable of forming heteromers, as the former are the major receptor forms detected after the pulse (see Fig. 2*A*), whereas only mature receptors are detectable after the 6-h chase (4). The HA-hδOR^{Phe-27} and the Myc-hδOR^{Cys-27}-FLAG variants were immunoprecipitated from the cellular lysates using HA and FLAG antibodies, respectively, and after denaturation the co-immunoprecipitated receptors were pulled down in a second immunoprecipitation step using the appropriate antibodies. As a control, equal aliquots of the first immunoprecipitates were subjected to immunoprecipitation with the immobilized mouse IgG. As seen in Fig. 6*A*, the FLAG antibody pulled down the Cys-27 variant precursor forms, carrying either one or two *N*-glycans, from the HA antibody immunoprecipitate (compare *lanes 3* and *5*), and similarly, the HA antibody precipitated the 43-kDa Phe-27 precursor carrying two *N*-glycans from the FLAG antibody immunoprecipitate (compare *lanes 2* and *6*). No specific bands were found in the second immunoprecipitate if the mouse IgG was used (Fig. 6*A*, *lanes 1* and *4*). These results confirm that the two variants can heteromerize already in the ER and also suggest that both precursor glycoforms are capable of forming homo/heteromers. The results obtained using the 6-h chased samples were comparable with those obtained using the pulse-labeled ones (Fig. 6*B*), confirming that the mature variants also exit as homo/heteromers.

Finally, the homo/heteromerization of the hδOR variants was verified with a BRET assay using intact cells (Fig. 6*C*). This allowed demonstrating the specificity of the oligomerization *in vivo* without the detergent solubilization step that was required for the co-immunoprecipitation experiments. For the BRET assay, the hδOR variants were tagged at their C termini with *Renilla* luciferase (*R*luc) or a variant of the enhanced YFP (Venus). The Venus- and *R*luc-tagged receptors were then transiently co-transfected in HEK293 cells, and BRET titration experiments were performed. As seen in Fig. 6*C*, the titration curves for the different donor and acceptor pairs were best fitted to a hyperbolic function, and the calculated BRET$_{50}$ values that reflect the relative affinity between the donor and acceptor (48) were similar. This indicates that the variants have a similar propensity to form homomers and heteromers. Identical
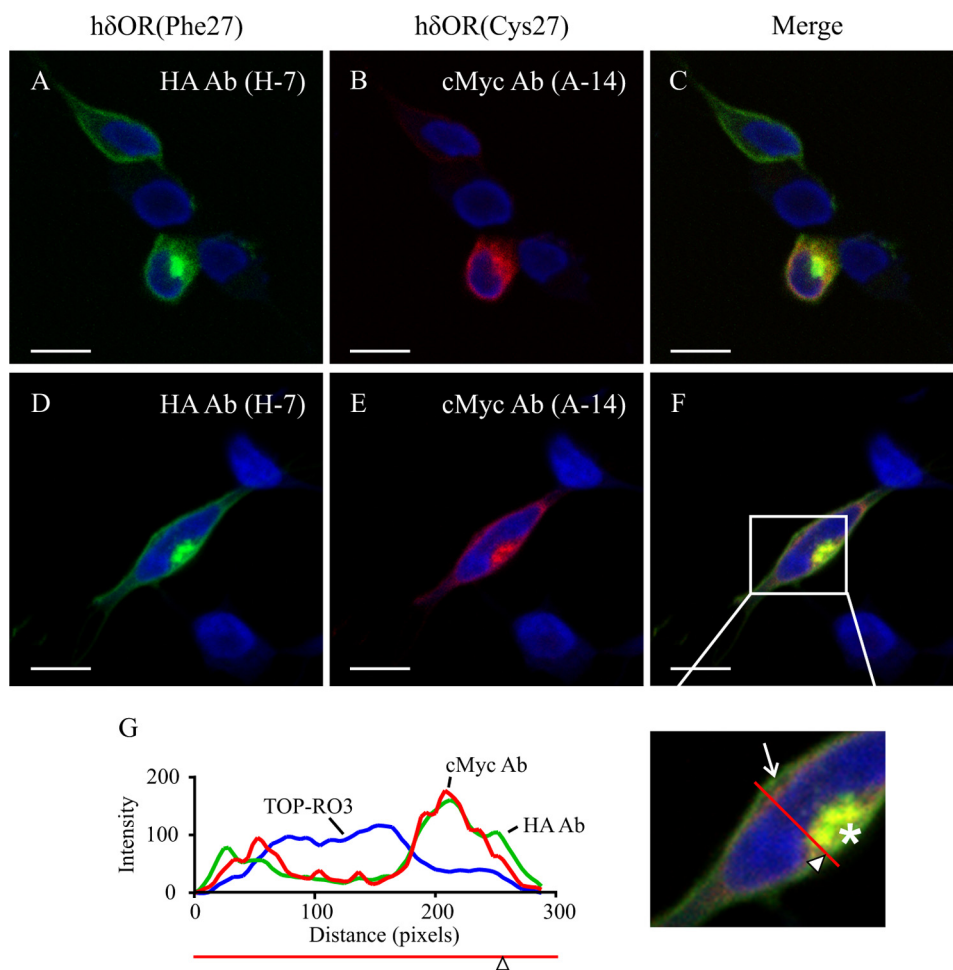
FIGURE 5. **Subcellular localization of hδOR^Cys-27 and hδOR^Phe-27 in transiently co-transfected SH-SY5Y neuroblastoma cells.** *A–F*, SH-SY5Y neuroblastoma cells were co-transfected with HA-hδOR^Phe-27 and Myc-hδOR^Cys-27-FLAG (1:2 ratio) for 24 h, and fixed cells were stained with HA (*green*) and cMyc (*red*) antibodies followed by Alexa Fluor 488/568 secondary antibodies, respectively. Nuclei were stained with TOP-RO3 iodide (*blue*). Cells were analyzed by confocal microscopy. For *panels A–C*, the transfection was performed under conditions that resulted in co-transfected cells or cells expressing only one of the variants. The *arrow* indicates plasma membrane receptors, and the *asterisk* intracellular receptor accumulation. The *red line* with an *arrowhead* indicates the line selection used for the RGB profile plot analysis shown in *panel G*. *Bars*, 10 μm.

results were obtained for the reciprocal constructs (data not shown), indicating that the position of the BRET donor and acceptor had no effect on the results. In addition, the specificity of the interaction was demonstrated by the lack of significant energy transfer under similar conditions when HA-hδOR^Phe-27-*R*luc was co-expressed with an unrelated receptor, the HA- and Venus-tagged glutamate receptor family member, GABA_B-R2 (Fig. 6*C*).

DISCUSSION

In recent years several studies have suggested that homo/heteromerization of GPCRs occurs constitutively before the receptors are inserted to the plasma membrane. This notion was originally thought to characterize only family C receptors but has now been extended to the largest GPCR subfamily, family A (also known as rhodopsin type GPCRs). The results shown in this study are in full agreement with this idea. We demonstrate that the hδOR Cys-27 variant that shows inherently compromised ER export impairs maturation and cell surface delivery of the co-expressed Phe-27 variant, leading to its enhanced targeting to ERAD. The ER-localized precursors, as well as the cell surface mature variants, were found to exist in homo/het-

eromers and no differences were observed in their ability to form these oligomeric complexes. The cellular expression level of each of the two variants thus governs the ratio of homo/heteromers. The hδOR F27C polymorphism may thus have functional consequences in heterozygous individuals that carry both variant forms, possibly relating to altered receptor expression levels and cellular responsiveness to the opioid ligand exposure.

A number of naturally occurring mutants and splice variants of family A GPCRs have previously been shown to cause ER retention of the corresponding wild-type receptors upon co-expression. For example, several rhodopsin mutants that cause autosomal dominant retinitis pigmentosa, redirect the wild-type protein to degradation when co-expressed in HEK293 cells (22). In this study, the impairment of hδOR^Phe-27 maturation and ER export in cells co-expressing the two hδOR variants was shown to be specifically mediated by the Cys-27 variant and was not because of overloading the capacity of the cells to handle overexpressed membrane proteins. No induction of the unfolded protein response was observed and no impairment in maturation of the endogenously expressed transferrin receptor
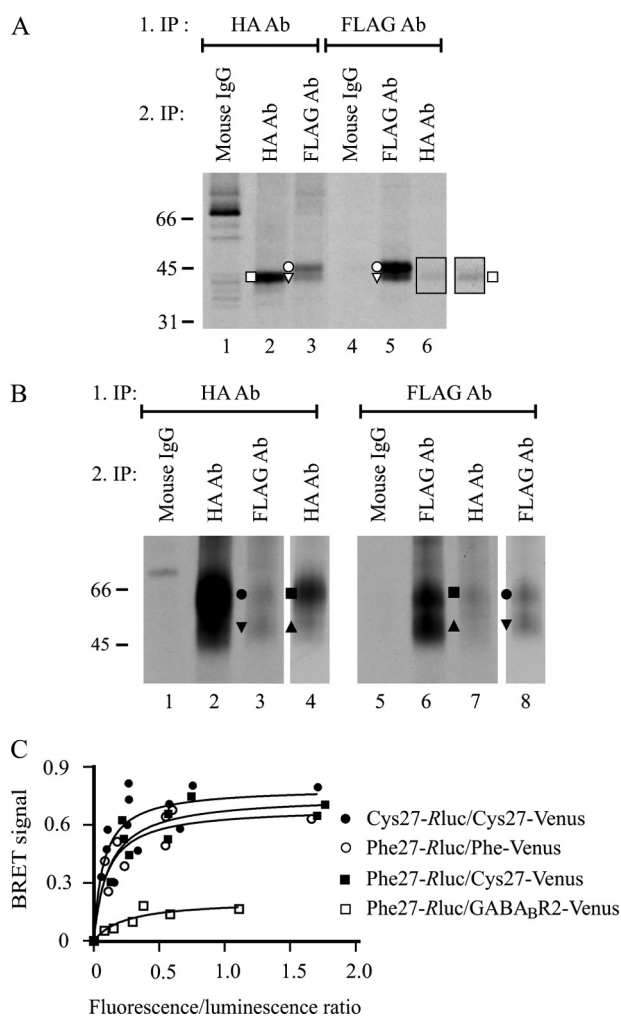
A

B

C

FIGURE 6. **Both precursor and mature receptor forms of hδOR^Cys-27 and hδOR^Phe-27 variants form homo/heteromers.** *A* and *B*, co-immunoprecipitation. HEK293$_i$ cells constitutively expressing HA-hδOR^Phe-27 were induced to express Myc-hδOR^Cys-27-FLAG, pulse-labeled with [^{35}S]methionine/cysteine for 40 min, and harvested immediately (*A*) or chased for 6 h (*B*). Receptors were purified from cellular lysates by sequential immunoprecipitation, performing the first step in native conditions with the FLAG M2 or HA antibody. Proteins were eluted with SDS-containing buffer, and re-immunoprecipitation was performed from the diluted denatured eluates with the FLAG M2 or HA antibodies or the mouse IgG, as indicated. Only one-eighth and one-fourth of the samples was loaded on *lanes 2* and *5* in *panel A* and on *lanes 2* and *6* in *panel B*, respectively. In *panel A*, the outlined squared area of *lane 6* is shown with enhanced contrast. In *panel B*, the *lanes 4* and *8* represent shorter exposures of *lanes 2* and *6*, respectively. The precursor and mature receptor forms are indicated with *open* and *closed symbols*, respectively, as specified in Fig. 1. The difference in migration of the 2-*N*-glycan precursors of the two variants (*A*) is because of the distinct N- and C-terminal tags. *C*, BRET measurements. HEK293 cells were transiently co-transfected with different amounts of energy donors (hδOR^Cys-27-*R*luc, hδOR^Phe-27-*R*luc) and energy acceptors (HA-hδOR^Cys-27-Venus, HA-hδOR^Phe-27-Venus, HA-GABA$_B$R2-Venus) as indicated. After 48 h, BRET signals were measured after the addition of the luciferase substrate coelenterazine H. The results shown are plotted as a function of the ratio of total fluorescence (Venus) and total luminescence (*R*luc) and are representative of two independent experiments carried out in duplicate. The curves were fitted using a non-linear regression analysis with a single binding site.

was detected in the co-transfected HEK293 cells. Furthermore, overexpression of the rat LHR that shows similar impaired ER export as hδOR^Cys-27 (38) had no effect on hδOR^Phe-27 maturation in the co-transfected human SH-SY5Y neuroblastoma cells. These results thus indicate that not only fully folding incompetent mutant receptors but also receptor forms that

have relatively subtle difficulties in folding/ER export can act in a dominant negative manner and lead to a decreased cell surface expression of the corresponding "wild-type" receptors. This underscores the importance of the stringent ER quality control mechanisms that scrutinize newly synthesized proteins and, furthermore, raises the question whether a similar dominant negative effect is a more general characteristic of common GPCR polymorphic variants than has been anticipated.

The dominant negative effects of mutant receptors on their wild-type counterparts have been taken as evidence that GPCR homo/heteromerization occurs intracellularly. This study provides ample evidence that this is the case for δOR when considering both the physical interactions between hδOR^Phe-27 and hδOR^Cys-27 and the influence of their co-expression on the maturation profile of hδOR^Phe-27. Co-expression of the two receptor variants in either the HEK293 or SH-SY5Y cells led to an intracellular accumulation of the hδOR^Phe-27 precursors with a concomitant decrease in the number of mature receptors at the cell surface. This was shown by metabolic labeling, Western blotting, and flow cytometry as well as by confocal microscopy. In addition, the co-expression led to an enhanced targeting of hδOR^Phe-27 precursors to ERAD, as they were stabilized in cells treated with a proteasomal inhibitor lactacystin. The treatment also resulted in an increase in the amount of polyubiquitinated receptors. Furthermore, maturation of the ER-retained precursors was rescued by a membrane-permeable opioid antagonist naltrexone that is known to act intracellularly as a pharmacological chaperone for hδOR (4, 5).

More direct evidence supporting the notion that the hδOR oligomeric complexes form shortly after synthesis was provided by the sequential co-immunoprecipitation experiments. Using metabolically labeled cells and differentially epitope-tagged variants, we were able to demonstrate that the receptor precursors exist as heteromers. The use of metabolically labeled cells was a clear advantage because it allowed the independent investigation of ER-localized precursors and mature cell surface receptors and the use of sequential immunoprecipitation. Previous co-immunoprecipitation studies on opioid receptors have relied mostly on Western blotting techniques (8, 9, 49), which do not equivocally allow discrimination between intracellular biosynthetic intermediates and cell surface proteins. Furthermore, the two-step immunoprecipitation used in this study was performed in more stringent conditions than the one-step co-immunoprecipitations previously used for Western blot assays. The BRET measurements performed utilized intact cells and could, therefore, not distinguish, in which cellular compartment the variant homo/heteromers were located. Previously, the BRET technique has been successfully combined with subcellular fractionation, demonstrating that GPCR homo/heteromerization is detectable in ER membrane fractions (11, 50, 51). Similarly, specific BRET signals between β_1-adrenergic receptors were detected in cells that were treated with brefeldin A (36), a drug that collapses the Golgi and impairs ER export of newly synthesized proteins. Furthermore, mutations in the β_1-adrenergic receptors that impair dimerization were found to lead receptor retention in the ER (36).

Co-expression of Human δ-Opioid Receptor F27C Variants

The quantitative changes in the expression of hδOR[Phe-27] precursors and mature forms that were observed in the co-transfected HEK293 cells were accompanied by alterations in the appearance of different receptor glycoforms. We have shown previously that *N*-glycosylation of Asn-33 in the N-terminal domain of hδOR[Cys-27] is inefficient, leading to expression of two glycoforms carrying either one or two *N*-glycans attached to Asn-18 or Asn-18/Asn-33, respectively (44). In contrast, the Phe-27 variant, when expressed alone, is *N*-glycosylated efficiently at both sites (4). The co-expression, surprisingly, led to an increase in the relative amount of hδOR[Phe-27] precursors and mature forms carrying only one *N*-glycan. No apparent changes were observed in glycosylation of the endogenously expressed transferring receptor. These observations support the assumption that homo/heteromerization of the hδOR variants occurs very early after synthesis, even co-translationally. It can be hypothesized that the specific changes in *N*-glycosylation of the Phe-27 variant result from steric hindrance, possibly by a protein that interacts with the hδOR[Cys-27] N-terminal domain during or shortly after synthesis. We have suggested previously that such an interaction is likely to be the cause for ER accumulation of the Cys-27 variant after long term expression (4).

Importantly, the qualitative changes observed for the receptor glycoforms were accompanied by changes in apparent heterogeneity of the mature hδOR[Phe-27] forms on SDS-PAGE when the two variants were co-expressed. The most likely explanation for this observation is an altered processing of receptor *N*- and *O*-glycans in the Golgi, suggesting that the newly synthesized receptors, once having formed homo/heteromeric complexes in the ER, transit the Golgi to the plasma membrane in the oligomeric form. It can be hypothesized that the close proximity of receptor N termini after homo/heteromerization might sterically hinder the Golgi-localized glycosyltransferases. The existence of cell surface homo/heteromers of the hδOR variants was verified in the co-immunoprecipitation experiments, showing that not only the precursors but also the mature receptors existed as homo/heteromers. Whether these oligomeric complexes that reach the cell surface are stable or transient in nature remains to be investigated in the future.

The dynamic nature of cell surface opioid receptor oligomeric complexes is presently under extensive research, and no definitive consensus has been reached whether there is specific regulation of the homo/heteromers relating to receptor activation and internalization (for review, see Ref. 18). Studies on the possible functional consequences of the hδOR variant heteromers on receptor internalization will be especially important. The two variants show altered trafficking properties not only in the secretory pathway but also at the cell surface, as the Cys-27 variant appears to be unstable at the cell surface and is very prone to constitutive internalization (4). It is likely to be subject to cell surface quality control that disposes apparent membrane proteins to lysosomal degradation (52). In our recent study we demonstrated that hδOR F27C polymorphism might represent a risk factor for Alzheimer disease as heterozygotes were over-represented among the Alzheimer disease patients in two independent study populations. We also observed that overexpression of the Cys-27 variant, but not that of the Phe-27 one, caused major changes in processing of the exogenously or endogenously expressed amyloid precursor protein in SH-SY5Y and HEK293 cells (3). This occurred most likely via a mechanism that relates to the enhanced constitutive internalization of hδOR[Cys-27] (4). These results underscore the possibility that even common GPCR polymorphisms that are characterized by altered receptor trafficking may have unexpected consequences *in vivo*.

REFERENCES

1. Waldhoer, M., Bartlett, S. E., and Whistler, J. L. (2004) Opioid receptors. *Annu. Rev. Biochem.* **73,** 953–990
2. Gelernter, J., and Kranzler, H. R. (2000) Variant detection at the δ-opioid receptor (OPRD1) locus and population genetics of a novel variant affecting protein sequence. *Hum. Genet* **107,** 86–88
3. Sarajärvi, T., Tuusa, J. T., Haapasalo, A., Lackman, J. J., Sormunen, R., Helisalmi, S., Roehr, J. T., Parrado, A. R., Mäkinen, P., Bertram, L., Soininen, H., Tanzi, R. E., Petäjä-Repo, U. E., and Hiltunen, M. (2011) Cysteine 27 variant of the δ-opioid receptor affects amyloid precursor protein processing through altered endocytic trafficking. *Mol. Cell. Biol.* **31,** 2326–2340
4. Leskelä, T. T., Markkanen, P. M., Alahuhta, I. A., Tuusa, J. T., and Petäjä-Repo, U. E. (2009) Phe27Cys polymorphism alters the maturation and subcellular localization of the human δ-opioid receptor. *Traffic* **10,** 116–129
5. Petäjä-Repo, U. E., Hogue, M., Bhalla, S., Laperrière, A., Morello, J. P., and Bouvier, M. (2002) Ligands act as pharmacological chaperones and increase the efficiency of δ-opioid receptor maturation. *EMBO J.* **21,** 1628–1637
6. Leskelä, T. T., Markkanen, P. M., Pietilä, E. M., Tuusa, J. T., and Petäjä-Repo, U. E. (2007) Opioid receptor pharmacological chaperones act by binding and stabilizing newly synthesized receptors in the endoplasmic reticulum. *J. Biol. Chem.* **282,** 23171–23183
7. Cvejic, S., and Devi, L. A. (1997) Dimerization of the δ-opioid receptor. Implication for a role in receptor internalization. *J. Biol. Chem.* **272,** 26959–26964
8. Jordan, B. A., and Devi, L. A. (1999) G protein-coupled receptor heterodimerization modulates receptor function. *Nature* **399,** 697–700
9. McVey, M., Ramsay, D., Kellett, E., Rees, S., Wilson, S., Pope, A. J., and Milligan, G. (2001) Monitoring receptor oligomerization using time-resolved fluorescence resonance energy transfer and bioluminescence resonance energy transfer. The human δ-opioid receptor displays constitutive oligomerization at the cell surface, which is not regulated by receptor occupancy. *J. Biol. Chem.* **276,** 14092–14099
10. Ramsay, D., Kellett, E., McVey, M., Rees, S., and Milligan, G. (2002) Homo- and hetero-oligomeric interactions between G protein-coupled receptors in living cells monitored by two variants of bioluminescence resonance energy transfer (BRET). Hetero-oligomers between receptor subtypes form more efficiently than between less closely related sequences. *Biochem. J.* **365,** 429–440
11. Wang, D., Sun, X., Bohn, L. M., and Sadée, W. (2005) Opioid receptor homo- and heterodimerization in living cells by quantitative bioluminescence resonance energy transfer. *Mol. Pharmacol.* **67,** 2173–2184
12. Xie, Z., Bhushan, R. G., Daniels, D. J., and Portoghese, P. S. (2005) Interaction of bivalent ligand KDN21 with heterodimeric δ-κ-opioid receptors in human embryonic kidney 293 cells. *Mol. Pharmacol.* **68,** 1079–1086
13. Waldhoer, M., Fong, J., Jones, R. M., Lunzer, M. M., Sharma, S. K., Koste-

nis, E., Portoghese, P. S., and Whistler, J. L. (2005) A heterodimer-selective agonist shows *in vivo* relevance of G protein-coupled receptor dimers. *Proc. Natl. Acad. Sci. U.S.A.* **102,** 9050–9055

14. Breit, A., Gagnidze, K., Devi, L. A., Lagacé, M., and Bouvier, M. (2006) Simultaneous activation of the δ-opioid receptor (δ-OR)/sensory neuron-specific receptor-4 (SNSR-4) hetero-oligomer by the mixed bivalent agonist bovine adrenal medulla peptide 22 activates SNSR-4 but inhibits δOR signaling. *Mol. Pharmacol.* **70,** 686–696

15. Hasbi, A., Nguyen, T., Fan, T., Cheng, R., Rashid, A., Alijaniaram, M., Rasenick, M. M., O'Dowd, B. F., and George, S. R. (2007) Trafficking of preassembled opioid μ-δ heterooligomer-Gz signaling complexes to the plasma membrane. Coregulation by agonists. *Biochemistry* **46,** 12997–13009

16. Parenty, G., Appelbe, S., and Milligan, G. (2008) CXCR2 chemokine receptor antagonism enhances DOP opioid receptor function via allosteric regulation of the CXCR2-DOP receptor heterodimer. *Biochem. J.* **412,** 245–256

17. Gupta, A., Mulder, J., Gomes, I., Rozenfeld, R., Bushlin, I., Ong, E., Lim, M., Maillet, E., Junek, M., Cahill, C. M., Harkany, T., and Devi, L. A. (2010) Increased abundance of opioid receptor heteromers after chronic morphine administration. *Sci. Signal.* **3,** ra54

18. van Rijn, R. M., Whistler, J. L., and Waldhoer, M. (2010) Opioid receptor heteromer-specific trafficking and pharmacology. *Curr. Opin. Pharmacol.* **10,** 73–79

19. Rozenfeld, R., and Devi, L. A. (2011) Exploring a role for heteromerization in GPCR signalling specificity. *Biochem. J.* **433,** 11–18

20. Kniazeff, J., Prézeau, L., Rondard, P., Pin, J. P., and Goudet, C. (2011) Dimers and beyond. The functional puzzles of class C GPCRs. *Pharmacol. Ther.* **130,** 9–25

21. Bulenger, S., Marullo, S., and Bouvier, M. (2005) Emerging role of homo- and heterodimerization in G protein-coupled receptor biosynthesis and maturation. *Trends Pharmacol. Sci.* **26,** 131–137

22. Rajan, R. S., and Kopito, R. R. (2005) Suppression of wild-type rhodopsin maturation by mutants linked to autosomal dominant retinitis pigmentosa. *J. Biol. Chem.* **280,** 1284–1291

23. Karpa, K. D., Lin, R., Kabbani, N., and Levenson, R. (2000) The dopamine D3 receptor interacts with itself and the truncated D3 splice variant d3nf. D3-D3nf interaction causes mislocalization of D3 receptors. *Mol. Pharmacol.* **58,** 677–683

24. Lee, S. P., O'Dowd, B. F., Ng, G. Y., Varghese, G., Akil, H., Mansour, A., Nguyen, T., and George, S. R. (2000) Inhibition of cell surface expression by mutant receptors demonstrates that D2 dopamine receptors exist as oligomers in the cell. *Mol. Pharmacol.* **58,** 120–128

25. Grosse, R., Schöneberg, T., Schultz, G., and Gudermann, T. (1997) Inhibition of gonadotropin-releasing hormone receptor signaling by expression of a splice variant of the human receptor. *Mol. Endocrinol.* **11,** 1305–1318

26. Brothers, S. P., Cornea, A., Janovick, J. A., and Conn, P. M. (2004) Human loss-of-function gonadotropin-releasing hormone receptor mutants retain wild-type receptors in the endoplasmic reticulum. Molecular basis of the dominant-negative effect. *Mol. Endocrinol.* **18,** 1787–1797

27. Sánchez-Laorden, B. L., Sánchez-Más, J., Martínez-Alonso, E., Martínez-Menárguez, J. A., García-Borrón, J. C., and Jiménez-Cervantes, C. (2006) Dimerization of the human melanocortin 1 receptor. Functional consequences and dominant-negative effects. *J. Invest. Dermatol.* **126,** 172–181

28. Beaumont, K. A., Shekar, S. N., Shekar, S. L., Newton, R. A., James, M. R., Stow, J. L., Duffy, D. L., and Sturm, R. A. (2007) Receptor function, dominant negative activity, and phenotype correlations for MC1R variant alleles. *Hum. Mol. Genet.* **16,** 2249–2260

29. Calebiro, D., de Filippis, T., Lucchi, S., Covino, C., Panigone, S., Beck-Peccoz, P., Dunlap, D., and Persani, L. (2005) Intracellular entrapment of wild-type TSH receptor by oligomerization with mutants linked to dominant TSH resistance. *Hum. Mol. Genet* **14,** 2991–3002

30. Apaja, P. M., Tuusa, J. T., Pietilä, E. M., Rajaniemi, H. J., and Petäjä-Repo, U. E. (2006) Luteinizing hormone receptor ectodomain splice variant misroutes the full-length receptor into a subcompartment of the endoplasmic reticulum. *Mol. Biol. Cell* **17,** 2243–2255

31. Benkirane, M., Jin, D. Y., Chun, R. F., Koup, R. A., and Jeang, K. T. (1997) Mechanism of transdominant inhibition of CCR5-mediated HIV-1 infection by ccr5delta32. *J. Biol. Chem.* **272,** 30603–30606

32. Shioda, T., Nakayama, E. E., Tanaka, Y., Xin, X., Liu, H., Kawana-Tachikawa, A., Kato, A., Sakai, Y., Nagai, Y., and Iwamoto, A. (2001) Naturally occurring deletional mutation in the C-terminal cytoplasmic tail of CCR5 affects surface trafficking of CCR5. *J. Virol.* **75,** 3462–3468

33. Zhu, X., and Wess, J. (1998) Truncated V2 vasopressin receptors as negative regulators of wild-type V2 receptor function. *Biochemistry* **37,** 15773–15784

34. Hague, C., Uberti, M. A., Chen, Z., Hall, R. A., and Minneman, K. P. (2004) Cell surface expression of α1D-adrenergic receptors is controlled by heterodimerization with α1B-adrenergic receptors. *J. Biol. Chem.* **279,** 15541–15549

35. Canals, M., Lopez-Gimenez, J. F., and Milligan, G. (2009) Cell surface delivery and structural reorganization by pharmacological chaperones of an oligomerization-defective α (1b)-adrenoceptor mutant demonstrates membrane targeting of GPCR oligomers. *Biochem. J.* **417,** 161–172

36. Kobayashi, H., Ogawa, K., Yao, R., Lichtarge, O., and Bouvier, M. (2009) Functional rescue of β-adrenoceptor dimerization and trafficking by pharmacological chaperones. *Traffic* **10,** 1019–1033

37. Law, P. Y., Erickson-Herbrandson, L. J., Zha, Q. Q., Solberg, J., Chu, J., Sarre, A., and Loh, H. H. (2005) Heterodimerization of μ- and δ-opioid receptors occurs at the cell surface only and requires receptor-G protein interactions. *J. Biol. Chem.* **280,** 11152–11164

38. Pietilä, E. M., Tuusa, J. T., Apaja, P. M., Aatsinki, J. T., Hakalahti, A. E., Rajaniemi, H. J., and Petäjä-Repo, U. E. (2005) Inefficient maturation of the rat luteinizing hormone receptor. A putative way to regulate receptor numbers at the cell surface. *J. Biol. Chem.* **280,** 26622–26629

39. Tuusa, J. T., Leskelä, T. T., and Petäjä-Repo, U. E. (2010) Human δ-opioid receptor biogenesis is regulated via interactions with SERCA2b and calnexin. *FEBS J.* **277,** 2815–2829

40. Nagai, T., Ibata, K., Park, E. S., Kubota, M., Mikoshiba, K., and Miyawaki, A. (2002) A variant of yellow fluorescent protein with fast and efficient maturation for cell-biological applications. *Nat. Biotechnol.* **20,** 87–90

41. Villemure, J. F., Adam, L., Bevan, N. J., Gearing, K., Chénier, S., and Bouvier, M. (2005) Subcellular distribution of GABA(B) receptor homo- and heterodimers. *Biochem. J.* **388,** 47–55

42. Petaja-Repo, U. E., Hogue, M., Laperriere, A., Bhalla, S., Walker, P., and Bouvier, M. (2001) Newly synthesized human δ-opioid receptors retained in the endoplasmic reticulum are retrotranslocated to the cytosol, deglycosylated, ubiquitinated, and degraded by the proteasome. *J. Biol. Chem.* **276,** 4416–4423

43. Petäjä-Repo, U. E., Hogue, M., Leskelä, T. T., Markkanen, P. M., Tuusa, J. T., and Bouvier, M. (2006) Distinct subcellular localization for constitutive and agonist-modulated palmitoylation of the human δ-opioid receptor. *J. Biol. Chem.* **281,** 15780–15789

44. Markkanen, P. M., and Petäjä-Repo, U. E. (2008) *N*-Glycan-mediated quality control in the endoplasmic reticulum is required for the expression of correctly folded δ-opioid receptors at the cell surface. *J. Biol. Chem.* **283,** 29086–29098

45. Yang, B., Hoe, M. H., Black, P., and Hunt, R. C. (1993) Role of oligosaccharides in the processing and function of human transferrin receptors. Effect of the loss of the three *N*-glycosyl oligosaccharides individually or together. *J. Biol. Chem.* **268,** 7435–7441

46. Do, S. I., and Cummings, R. D. (1992) Presence of O-linked oligosaccharide on a threonine residue in the human transferrin receptor. *Glycobiology* **2,** 345–353

47. Levitt, E. S., Purington, L. C., and Traynor, J. R. (2011) $G_{i/o}$-coupled receptors compete for signaling to adenylyl cyclase in SH-SY5Y cells and reduce opioid-mediated cAMP overshoot. *Mol. Pharmacol.* **79,** 461–471

48. Mercier, J. F., Salahpour, A., Angers, S., Breit, A., and Bouvier, M. (2002) Quantitative assessment of β1- and β2-adrenergic receptor homo- and heterodimerization by bioluminescence resonance energy transfer. *J. Biol. Chem.* **277,** 44925–44931

49. George, S. R., Fan, T., Xie, Z., Tse, R., Tam, V., Varghese, G., and O'Dowd,

B. F. (2000) Oligomerization of μ- and δ-opioid receptors. Generation of novel functional properties. *J. Biol. Chem.* **275,** 26128–26135

50. Salahpour, A., Angers, S., Mercier, J. F., Lagacé, M., Marullo, S., and Bouvier, M. (2004) Homodimerization of the β2-adrenergic receptor as a prerequisite for cell surface targeting. *J. Biol. Chem.* **279,** 33390–33397

51. Terrillon, S., Durroux, T., Mouillac, B., Breit, A., Ayoub, M. A., Taulan, M., Jockers, R., Barberis, C., and Bouvier, M. (2003) Oxytocin and vasopressin V1a and V2 receptors form constitutive homo- and heterodimers during biosynthesis. *Mol. Endocrinol.* **17,** 677–691

52. Okiyoneda, T., Apaja, P. M., and Lukacs, G. L. (2011) Protein quality control at the plasma membrane. *Curr. Opin. Cell Biol.* **23,** 483–491